Journal of Sound and Vibration (2002) **249**(3), 499–527
doi:10.1006/jsvi.2001.3847, available online at http://www.idealibrary.com on IDEAL®

ANALYSIS OF THE FLEXURAL VIBRATION OF A THIN-PLATE BOX USING A COMBINATION OF FINITE ELEMENT ANALYSIS AND ANALYTICAL IMPEDANCES

R. M. GRICE AND R. J. PINNINGTON

Institute of Sound and Vibration Research, University of Southampton, Southampton, SO17 1BJ, England. E-mail: rm_grice@yahoo.com

(*Received* 19 *December* 2000, *and in final form* 30 *May* 2001)

Many practical built-up thin-plate structures, e.g., a modern car body, are essentially assemblies of numerous thin plates joined at their edges. The plates are so thin that they invariably support the weight of the structure and machinery using their substantial in-plane stiffness. Consequently, vibrational power injected into the structure from sources mounted at these stiff points is controlled by high impedance long-wavelength in-plane waves in the plates. As the long in-plane waves propagate around the structure, they impinge upon the numerous structural joints at which short-wavelength flexural waves are generated in adjoining plates. These flexural waves have much lower impedance than the in-plane waves. Hence, the vibration of thin-plate structures excited at their stiff points develops into a mixture of long in-plane waves and short flexural waves. In a previous paper by the same authors, a numerically efficient finite element analysis which accommodated only the long in-plane waves was used to predict the forced response of a six-sided thin-plate box at the stiff points. This paper takes that finite element analysis and, drawing on theory developed in two additional papers by the same authors, couples analytical impedances to it in order to represent the short flexural waves generated at the structural joints. The parameters needed to define these analytical impedances are identified. The vibration of the impedances are used to calculate estimates of the mean-square flexural vibration of the box sides which compare modestly with laboratory measurements. The method should have merit in predicting the vibration of built-up thin-plate structures in the so-called "mid-frequency" region where the modal density of the long waves is too low to allow confident application of statistical energy analysis, yet the modal density of the short flexural waves is too high to allow efficient finite element analysis.

1. INTRODUCTION

In a paper by the present authors [1], a method was given for the analysis of the plate-stiffened beam, a structure which consists of a stiff beam connected along one edge to a large flexible rectangular plate. The plate-stiffened beam is broadly representative of the machinery foundation of a ship whose stiff beam-like frames carry the main machinery loads. Consequently, the vibrational power injected into the machinery foundation is controlled by the impedance of long-wavelength waves in the frames. The waves in the frames propagate large distances because of their long wavelengths, thereby dictating the power transmitted through the structure. The frames are attached to numerous flexible plates which do not carry appreciable machinery loads but whose edges are excited by the long waves travelling along the stiff frames. Thus, short-wavelength flexural waves radiate into the flexible plates, removing power from the long waves and hence damping them. To introduce the terminology of reference [1], the frames are called the "spine"

0022-460X/02/030499 + 29 $35.00/0

because they control both the power input and the power transmission, whereas the plates are called the "receiver" because they receive vibrational power from the spine and not directly from machinery sources.

It was shown in reference [1] that the wavelength of the waves in the spine (i.e., the beam) is normally much greater than the wavelength of the waves in the receiver (i.e., the plate). Consequently it was demonstrated that, provided the spine waves are at least twice as long as the receiver waves, the receiver presents a *locally reacting impedance* to the spine, i.e., the waves in the receiver radiate almost normal to the spine axis [2]. Hence, it was shown that the equation of motion of the spine could be written as the equation of motion for a beam plus an additional term which represented the locally reacting receiver impedance. This equation of motion was used to a produce a closed-form expression for the forced response of a plate-stiffened beam consisting of an end-excited uniform beam attached to a rectangular plate. The resulting predictions agreed well with laboratory measurements.

In reference [3], the analytical approach of reference [1] was developed into a "hybrid" numerical and analytical method as follows. First, the spine was analyzed in isolation of the receiver using finite element analysis. Since the waves in the spine are long, this analysis was numerically efficient. Second, the locally reacting receiver was represented as a series of finite-width plate strips. It was shown that the impedance of these plate-strips could be expressed using a straightforward analytical expression, and the parameters defining the impedance were defined. Third, the finite element analysis and receiver impedances were coupled together using a standard sub-structuring procedure [4] to predict the response of the complete structure. The hybrid method was applied to the uniform beam connected to a rectangular plate and the resulting predictions agreed well with measurements. In addition, it was shown that the power injected into the plate-strips could be used to accurately predict the mean-square vibration of the plate. The advantage of the hybrid method over the analytical approach of reference [1] was then demonstrated by accurately predicting the response of a plate-stiffened beam consisting of a uniform beam attached to a trapezoidally shaped plate, a structure whose response cannot be predicted in closed form.

In a third paper by the present authors [5], the forced response of a six-sided thin-plate box was analyzed using a finite element model which accommodates only in-plane motion. The motivation for this model comes from observations of the dynamic behaviour of built-up thin-plate structures like car bodies whose plates are so thin that they can only support static and dynamic loads using their massive in-plane stiffness. Consequently, the vibrational power injected into such a structure is controlled by the impedance of long-wavelength in-plane waves. As these waves propagate around the structure they generate short-wavelength flexural waves at the structural joints. These short waves radiate into the plates, thereby damping the long waves. In reference [5] it was shown that, under certain circumstances, it is possible to calculate the vibration of the built-up plate structure using only the long in-plane waves, in which case a finite element model which accommodates only in-plane motion is appropriate.

However, more fundamentally it is clear that the plate-stiffened beam and the six-sided box share the same overall spine and receiver characteristics, except for one important difference. In the plate-stiffened beam, the long and short waves travel in *separate* structural elements (the beam and plate respectively); in the six-sided box the long and short waves travel in the *same* structural element (collectively all the box plates). Reference [3] demonstrated how the hybrid method is applied to the first class of structure; the objective of this paper is to illustrate how the hybrid method can be used to predict the short-wavelength flexural vibrations in the second class of structure using the six-sided box as a test case. The procedure adopted, which is essentially the same as used in reference [3],

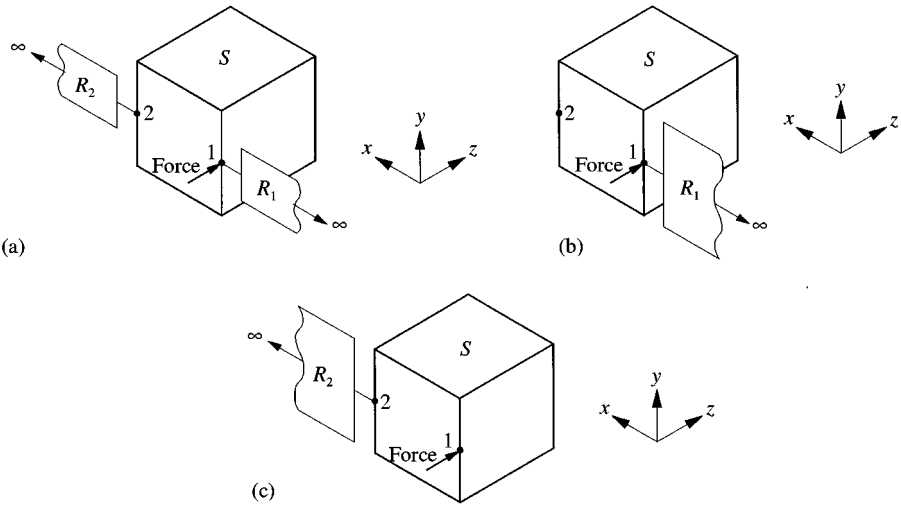

Figure 1. The thin-plate box (the spine S) coupled to analytical impedances (the receivers R) to form (a) compound, (b) parallel, and (c) series spine/receiver systems.

is illustrated in Figure 1 by the box S connected to two receivers R_1 and R_2 (the exact details of Figure 1 such as the choice of the receivers and their points of attachment are not important at this stage and will be explained fully in section 3). The method consists of three steps. First, the finite element model from [5] is used to predict the long-wave response at the stiff joints around the spine S. Second, analytical impedances (R_1 and R_2 in Figure 1) are calculated which model the impedance of short flexural waves generated at the joints by the long waves. Third, a sub-structuring procedure [3] is used to couple the finite element model to the analytical impedances, thereby predicting the response of the structure due to both waves types.

The layout of this paper is as follows. Section 2 presents theory which answers some very general questions concerning the parameters required to describe the receivers (such as their impedance and the damping which they produce when attached to the spine). Section 3 tests the theory from section 2 by considering the case of the box attached to either one or two receivers (as in Figure 1). This shows that the location of the receivers on the spine is an additional parameter. Section 4 then investigates the receiver location parameter by coupling greater numbers of receivers than shown in Figure 1 to the box. Finally, section 5 constructs a hybrid model for the box which uses the receiver vibration to estimate the mean-square response of the box sides. This estimate is compared with laboratory measurements.

Overall, it is considered that the hybrid method should be beneficial in predicting the vibration of built-up thin-plate structures in the so-called "mid-frequency" region where the modal density of the long waves is too low to allow confident application of statistical energy analysis, yet the modal density of the short flexural waves is too high to allow efficient finite element analysis.

2. GENERAL RECEIVER PARAMETERS

This section provides answers to two general questions relating to the receivers. First, over what frequency range are receivers required to model the impedance of flexural waves

generated at structural joints? Second, what is the relationship between the receiver impedance and the damping which they produce when attached to the spine?

2.1. THE FREQUENCY RANGE OVER WHICH RECEIVERS ARE REQUIRED

In reference [5], it was shown that there is a power balance between the time-averaged power injected into the structure at its stiff joints $\bar{P}_{IN}$, the inherent damping of the long waves and the power transmitted to the short waves at the joints. In reference [5] this was written as

$$\bar{P}_{IN} = \eta_I \omega \bar{E}_I + \eta_F \omega \bar{E}_F, \tag{1}$$

where $\eta_I \omega \bar{E}_I$ is the power dissipated by the inherent damping of the long waves having loss factor η_I and $\bar{E}_I$ is their vibrational energy (a list of symbols is given in the appendix)

$$\bar{E}_I = \|\tilde{v}_I\|^2 (6 m_p'' L^2), \quad m_p'' = \rho t. \tag{2}$$

In equation (2), $\|\tilde{v}_I\|^2$ is the spatially averaged mean-square velocity of the long waves and $6 m_p'' L^2$ is the mass of the box having an average joint length L. The second term in equation (1) can be written [5] as

$$\eta_F \omega \bar{E}_F = \|\tilde{v}_I\|^2 \ \mathrm{Re}\{24 L \tilde{Z}_F'\}, \tag{3}$$

where $\tilde{Z}_F'$ is the *line impedance* (i.e., the impedance per unit joint width) of the flexural waves generated at the joints, and $24\,L$ is the total joint length of the box. This represents the condition in which all the edges of the box vibrate independently of one another, and occurs at high frequencies when the flexural wavelength is short in comparison with the overall dimensions of the box. At lower frequencies, the edges of the plates will become increasingly coupled in flexure, and the effective independent joint length will be somewhat less than $24\,L$.

Due to the large difference in the wavelength of the long and short waves in the structure demonstrated in reference [5], the line impedance can be estimated using the *locally reacting* impedance per unit width of a semi-infinite beam [1, 3]

$$\tilde{Z}_F' = \frac{m_p'' \omega}{2 k_{FI}} (1 + \mathrm{j}), \tag{4}$$

where k_{FI} is the wavenumber for flexural waves travelling in a uniform thin plate

$$k_{FI} = \sqrt{\omega} \left(\frac{m_p''}{D_{FI}} \right)^{1/4}, \quad D_{FI} = \frac{E t^3}{12(1 - \nu^2)}. \tag{5}$$

Note that the impedance of equation (4) ignores the moment restraint at the edges of the box which means that it is the lowest possible for a beam in flexure. It has been chosen for convenience presently and does not exclude other impedances if considered appropriate.

Hence, it was shown in reference [5] that there is a frequency $f_{I=F}$ at which the power dissipated by the in-plane waves equals the power transmitted to the flexural waves

at the joints

$$f_{I=F} = \frac{2}{\pi \eta_I^2 L^2} \sqrt{\frac{D_{FI}}{m_p''}}. \tag{6}$$

This frequency is important because below it the power transmitted to the flexural waves at joints is larger than the power dissipated by the in-plane waves. Thus, below $f_{I=F}$ receivers are required in the hybrid analysis of built-up thin-plate structures in order to adequately model the dominant power dissipation mechanism.

In the case of the box in reference [5], the in-plane wave loss factor was 0·05 giving $f_{I=F} = 4{\cdot}9$ kHz, although measurements suggested that this was an overestimate. For the purposes of this paper, to make the effect of the receivers more pronounced below this frequency, the in-plane wave loss factor is artificially reduced to 0·002 in sections 2–4, which means according to equation (6) that the power transmitted to the receivers will be even more important in damping the box below 4·9 kHz. For convenience, Figure 2(a) and 2(b) shows the input accelerance (ratio of acceleration to force) for the box in the z-direction at point 1 in Figure 1, calculated using the finite element model from reference [5] using in-plane motion only for in-plane loss factors of 0·05 and 0·002 (the material properties used are $E = 4{\cdot}7$ GN/m^2, $\rho = 1192$ kg/m^3, $v = 0{\cdot}3$ and the plate thickness is 5 mm). Figure 2(c) and 2(d) shows the transfer accelerance at point 2 in the z-direction in Figure 1. Sections 2–4 will demonstrate how receivers attached to the box are used to model the flexural waves generated at its joints, thereby increasing the damping of the lightly damped frequency response functions shown in Figure 2 above 0·002. Section 5 will then show how the power transmitted to the receivers at the joints is used to predict the spatially averaged mean-square response of the sides of the actual structure having the more heavily damped frequency response functions in Figure 2 from reference [5] whose in-plane loss factor is 0·05.

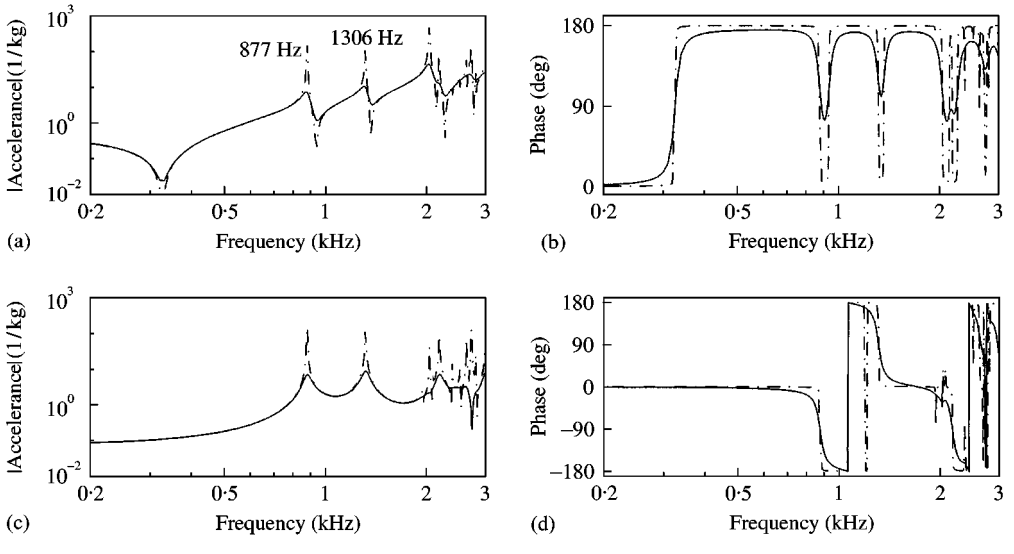

Figure 2. Response of the perspex box calculated using the membrane model with different loss factors of 0·05 (——) and 0·002 (– · – · –): (a, b), modulus and phase, respectively, of input accelerance at point 1 in the z-direction; (c, d), modulus and phase, respectively, of transfer accelerance at point 2 in z-direction.

2.2. THE RELATIONSHIP BETWEEN THE RECEIVER IMPEDANCE AND THE DAMPING WHICH THEY PRODUCE WHEN ATTACHED TO THE SPINE

Equation (6) determined when receivers are required in the hybrid method. This section shows the relationship between the receiver impedances and the damping which they produce when attached to the spine.

Returning to equation (1), and writing the term $\eta_F \omega \bar{E}_F$ in the form

$$\eta_F \omega \bar{E}_F = \|\tilde{v}_I\|^2 \,\mathrm{Re}\{N_R L_R \tilde{Z}'_F\}, \tag{7}$$

where N_R is the number of receivers attached to the spine and L_R is the total width of the receivers, the power injected into the structure is

$$\bar{P}_{IN} = \omega \bar{E}_I \left(\eta_I + \frac{N_R L_R \mathrm{Re}\{\tilde{Z}'_F\}}{\omega M_S} \right), \tag{8}$$

where M_S is the spine mass. The second term in the parentheses is a loss factor

$$\eta_F = \frac{N_R L_R \,\mathrm{Re}\{\tilde{Z}'_F\}}{\omega M_S}, \tag{9}$$

which defines how much damping is produced by attaching a certain number of receivers having a certain impedance. Using the impedance of equation (4), it can be seen that the additional damping produced by the receivers is greatest at low frequencies as expected from section 2.1. Equation (9) contains parameters N_R, L_R and $\tilde{Z}'_F$, values for which are determined in sections 3 and 4.

3. DETERMINATION OF RECEIVER PARAMETERS N_R AND L_R

Figure 1 shows the box attached to either one or two receivers R_1, R_2, but in general the spine S could be any built-up thin-plate structure which is excited at its stiff points. The spine is driven at point 1 by a force source $\tilde{f}_1$. In Figure 1(a) this force drives the spine in parallel with the receiver R_1 which is therefore called the *parallel receiver*. Receiver R_2 is attached to the spine at any point other than that at which the force acts and is called the *series receiver*.

Figure 1(a) is the general case of two simpler systems shown in Figure 1(b) and 1(c). The first of these shows only a parallel receiver and the second shows only a series receiver. The arrangement in Figure 1(a) is called the *compound system*. It might be necessary to attach more than two receivers to the spine or it might be necessary to attach only a single receiver. The motivation for the following analysis is to deduce, if possible, the *minimum* number of receivers which are required to damp it to a desired level, in order to minimize the amount of calculation. The compound system is analyzed because it is the most convenient general arrangement which can be analytically studied exactly. It allows one to observe the difference in the response between "one" and "more than one" receiver, thereby investigating the effect of varying N_R in equation (9). The receivers in Figure 1(a) are narrower than the receivers in Figure 1(b) and 1(c) in order to vary the receiver width L_R. Sections 3.1–3.4 study the effect of varying N_R and section 3.5 studies the effect of varying L_R.

3.1. COUPLED MATRIX FOR THE COMPOUND SYSTEM

In this section, the mobility matrix for the spine attached to the two receivers in Figure 1(a) is derived. This coupled mobility matrix will be used to compare and contrast the responses of all three systems shown in the figure.

Initially, consider the spine driven in isolation of the receivers at points 1 and 2 by two forces $\tilde{f}_1^S$ and $\tilde{f}_2^S$. The velocities at the points are related to these forces by

$$\begin{bmatrix} \tilde{v}_1^S \\ \tilde{v}_2^S \end{bmatrix} = \begin{bmatrix} \tilde{S}_1 & \tilde{S}_{12} \\ \tilde{S}_{21} & \tilde{S}_2 \end{bmatrix} \begin{bmatrix} \tilde{f}_1^S \\ \tilde{f}_1^S \end{bmatrix}, \tag{10}$$

where the quantities in the square matrix represent the input and transfer mobilities of the spine. A similar equation can be written for the two receivers

$$\begin{bmatrix} \tilde{v}_1^{R_1} \\ \tilde{v}_2^{R_2} \end{bmatrix} = \begin{bmatrix} \tilde{R}_1 & 0 \\ 0 & \tilde{R}_2 \end{bmatrix} \begin{bmatrix} \tilde{f}_1^{R_1} \\ \tilde{f}_1^{R_2} \end{bmatrix}, \tag{11}$$

where $\tilde{f}_1^{R_1}$ is the force acting on the parallel receiver at point 1 when it is uncoupled from the spine and $\tilde{R}_1$ is the parallel receiver input mobility (similarly for $\tilde{f}_1^{R_2}$ and $\tilde{R}_2$).

Since both these equations are of order 2 they can be inverted explicitly to produce for the spine

$$\begin{bmatrix} \tilde{f}_1^S \\ \tilde{f}_2^S \end{bmatrix} = \frac{1}{|\tilde{\mathbf{S}}|} \begin{bmatrix} \tilde{S}_1 & -\tilde{S}_{12} \\ -\tilde{S}_{21} & \tilde{S}_2 \end{bmatrix} \begin{bmatrix} \tilde{v}_1^S \\ \tilde{v}_2^S \end{bmatrix}, \tag{12}$$

and for the receivers

$$\begin{bmatrix} \tilde{f}_1^{R_1} \\ \tilde{f}_1^{R_2} \end{bmatrix} = \frac{1}{|\tilde{\mathbf{R}}|} \begin{bmatrix} \tilde{R}_2 & 0 \\ 0 & \tilde{R}_1 \end{bmatrix} \begin{bmatrix} \tilde{v}_1^{R_1} \\ \tilde{v}_1^{R_2} \end{bmatrix}, \tag{13}$$

where $|\tilde{\mathbf{S}}|, |\tilde{\mathbf{R}}|$ are the determinants of the spine and receiver mobility matrices, respectively,

$$|\tilde{\mathbf{S}}| = \tilde{S}_1\tilde{S}_2 - \tilde{S}_{12}\tilde{S}_{21}, \quad |\tilde{\mathbf{R}}| = \tilde{R}_1\tilde{R}_2. \tag{14}$$

To couple the spine and the two receivers, the following conditions are used:

$$\begin{bmatrix} \tilde{f}_1^C \\ 0 \end{bmatrix} = \begin{bmatrix} \tilde{f}_1^S \\ \tilde{f}_2^S \end{bmatrix} + \begin{bmatrix} \tilde{f}_1^{R_1} \\ \tilde{f}_1^{R_2} \end{bmatrix}, \quad \begin{bmatrix} \tilde{v}_1^C \\ \tilde{v}_2^C \end{bmatrix} = \begin{bmatrix} \tilde{v}_1^S \\ \tilde{v}_2^S \end{bmatrix} = \begin{bmatrix} \tilde{v}_1^{R_1} \\ \tilde{v}_1^{R_2} \end{bmatrix}, \tag{15}$$

where the superscript C indicates the forces and velocities present in the coupled structure. The coupled impedance matrix is then found to be

$$\tilde{\mathbf{Z}}^C = \frac{1}{|\tilde{\mathbf{S}}|} \begin{bmatrix} \tilde{S}_2 + \tilde{R}_2 \dfrac{|\tilde{\mathbf{S}}|}{|\tilde{\mathbf{R}}|} & -\tilde{S}_{12} \\ -\tilde{S}_{21} & \tilde{S}_1 + \tilde{R}_1 \dfrac{|\tilde{\mathbf{S}}|}{|\tilde{\mathbf{R}}|} \end{bmatrix}. \tag{16}$$

The coupled mobility matrix is found by inverting the coupled impedance matrix. After a little manipulation the coupled mobility matrix is found to be

$$\tilde{\mathbf{Y}}^C = \frac{1}{\tilde{\Delta}_1}\begin{bmatrix} \tilde{S}_1 + \tilde{R}_1\dfrac{|\tilde{\mathbf{S}}|}{|\tilde{\mathbf{R}}|} & \tilde{S}_{12} \\ \tilde{S}_{21} & \tilde{S}_2 + \tilde{R}_2\dfrac{|\tilde{\mathbf{S}}|}{|\tilde{\mathbf{R}}|} \end{bmatrix}, \quad \tilde{\Delta}_1 = 1 + \frac{|\tilde{\mathbf{S}}|}{|\tilde{\mathbf{R}}|} + \frac{\tilde{S}_1}{\tilde{R}_1} + \frac{\tilde{S}_2}{\tilde{R}_2}. \tag{17}$$

Two observations about (17) can be made:

(i) The compound system reduces to the parallel system merely by allowing the series receiver mobility $\tilde{R}_2$ to tend to infinity, i.e., by allowing its impedance to tend to zero. Similarly, the compound system reduces to the series system when $\tilde{R}_1 \to \infty$.

(ii) If the input mobility of any receiver falls below the spine input mobility at its point of attachment (i.e., the receiver impedance exceeds that of the spine), the coupled mobility matrix will differ significantly from the spine mobility matrix. Thus, if the spine mobility is to remain dominant

$$\tilde{\Delta}_1 \approx 1 \Rightarrow \frac{|\tilde{\mathbf{S}}|}{|\tilde{\mathbf{R}}|} \ll 1 \quad \text{and} \quad \frac{\tilde{S}_x}{\tilde{R}_x} \ll 1. \tag{18}$$

In the last ratio, x is any location on the spine at which a receiver is attached.

The implication of this result for the application of the hybrid method to built-up thin-plate structures in which both long and short waves travel in the same structural component is that the spine impedance must always exceed that of the receivers at the points at which they are attached to it. This ensures that the spine impedance always dominates the coupled response as required by reference [5]. This condition is only required for structures like the perspex box in which the single component (collectively all the plates) carries both wave types. It does not apply to structures like the plate-stiffened beam in which the waves travel in separate components. The condition is "one-sided" because the spine impedances must always exceed the receiver impedances at the points of attachment which can only be satisfied if $\tilde{\Delta}_1$ is approximately unity. Therefore, $\tilde{\Delta}_1$ could be used to define limits on the receiver impedances used in equation (9). Unfortunately, $\tilde{\Delta}_1$ requires the calculation of the determinant of two matrices. It will be shown shortly that there is a simpler criterion which can be applied to define the receiver impedances.

3.2. COUPLED MOBILITY MATRIX FOR A MODAL SPINE

In reference [5], the spine response was calculated by finite element analysis in which case its frequency response functions are based on a modal summation [6]

$$\tilde{S}_{jk} = \sum_{n=1}^{\infty} \Phi_{jn}\Phi_{kn}\tilde{S}_n, \tag{19}$$

where j, k are the input (e.g., force) and output (e.g., velocity) points on the spine, respectively, Φ_{jn}, Φ_{kn} are the values of the n-th mode shape at these two points and $\tilde{S}_n$ is the modal mobility function of the n-th mode

$$\tilde{S}_n = \frac{\mathrm{j}\omega\tilde{A}_n}{(\tilde{K}_n - M_n\omega^2)}, \quad (\tilde{A}_n = \text{a constant}). \tag{20}$$

If the spine is lightly damped and its resonances are well spaced (which is likely to be true since the waves in the spine are generally very long), the response of the spine in the region of any one resonance is dominated by that resonance and the input and transfer frequency response functions can be approximated by

$$\tilde{S}_1 \approx \Phi_{1p}^2 \tilde{S}_p, \quad \tilde{S}_2 \approx \Phi_{2p}^2 \tilde{S}_p, \quad \tilde{S}_{12} = \tilde{S}_{21} \approx \Phi_{1p}\Phi_{2p}\tilde{S}_p. \tag{21a–c}$$

Inserting these into the coupled mobility matrix of equation (17) yields

$$\tilde{\mathbf{Y}}_C \approx \frac{1}{\tilde{\Delta}_1}\begin{bmatrix} \tilde{S}_1 & \tilde{S}_{12} \\ \tilde{S}_{21} & \tilde{S}_2 \end{bmatrix}, \quad |\tilde{\mathbf{S}}| \approx 0, \quad \tilde{\Delta}_1 \approx 1 + \frac{\tilde{S}_1}{\tilde{R}_1} + \frac{\tilde{S}_2}{\tilde{R}_2}. \tag{22}$$

Two observations on equation (22) can be made

(i) For the parallel system, $\tilde{R}_2 \to \infty$ and hence

$$\tilde{\Delta}_1 \text{ (parallel)} \approx 1 + \frac{\tilde{S}_1}{\tilde{R}_1}. \tag{23}$$

For the series system, $\tilde{R}_2 \to \infty$ and therefore

$$\tilde{\Delta}_1 \text{ (series)} \approx 1 + \frac{\tilde{S}_2}{\tilde{R}_2}. \tag{24}$$

Now, if the spine is symmetric which is true for certain sets of locations on the box and which is approximately true for practical built-up thin-plate structures like car bodies manufactured from uniformly thin plates, one can say that $\tilde{S}_1 \approx \tilde{S}_2$ and $\tilde{R}_1 \approx \tilde{R}_2 = \tilde{R}$. Then for both the parallel and series systems

$$\tilde{\Delta}_1 \approx 1 + \frac{\tilde{S}_1}{\tilde{R}}, \tag{25}$$

and the coupled mobility matrices are the same for both the parallel and series systems.

(ii) For the compound system, if the spine is symmetric and the receivers are identical but have *half* the impedance of the receivers used in the parallel and series systems (i.e., they have twice the mobility) such that $\tilde{R}_1 = \tilde{R}_2 = 2\tilde{R}$, then $\tilde{\Delta}_1$ and the coupled mobility matrix are identical to case (i).

These observations suggest that for a lightly damped symmetric or near-symmetric spine vibrating at or close to a single well-spaced resonance, the response of that resonance can be damped by attaching a *single receiver at any point* on the structure. Alternatively, the resonance can be damped to the same degree by attaching *multiple receivers* provided the total impedance of these receivers equals that of the single receiver just mentioned. However, there is an obvious restriction on the location of the receivers which is that they must not be attached at vibration nodes of the particular mode shape in question. If any receiver is attached at a vibration node it will have little or no effect on the spine. Therefore, the location of the receivers is an additional parameter which will be elaborated upon in section 3.4.

Away from the frequency range in which any single resonance dominates the spine response, it is not straightforward to quantify the effect of the different receiver

configurations on the spine because the response is the result of a number of modes. However, this is not considered to be a serious shortcoming since one is normally interested in the damping in the region of spine resonances.

3.3. COUPLED MOBILITY MATRIX FOR A WAVE-BEARING SPINE

In the previous section the spine was assigned mobilities based on a modal model. In contrast, this section considers the response of the spine in the three configurations of Figure 1 when the spine input and transfer mobilities are described by wavefunctions. This is useful because the response of real structures is due to waves.

A simple wave-bearing system is a finite symmetric rod of length L carrying wavenumber $\tilde{k}_L$ having input and transfer mobilities [7]

$$\tilde{S}_1 = \tilde{S}_2 = S^\infty \frac{1+\tilde{\alpha}}{1-\tilde{\alpha}}, \quad \tilde{S}_{12} = \tilde{S}_{21} = S^\infty \frac{2\sqrt{\tilde{\alpha}}}{1-\tilde{\alpha}}, \quad \tilde{\alpha} = \mathrm{e}^{-\mathrm{j}2\tilde{k}_L L}, \quad \tilde{k}_L = \omega\sqrt{\frac{E}{\rho}}\left(1 - \mathrm{j}\frac{\eta}{2}\right), \tag{26}$$

where S^∞ is the characteristic mobility. Inserting these expressions into the coupled mobility matrix produces

$$\tilde{\mathbf{Y}}^C = \frac{1}{\tilde{\Delta}_1}\begin{bmatrix} \tilde{S}_1 + \tilde{R}_1\dfrac{(S^\infty)^2}{\tilde{R}_1\tilde{R}_2} & \tilde{S}_{12} \\ \tilde{S}_{21} & \tilde{S}_2 + \tilde{R}_2\dfrac{(\tilde{S}^\infty)^2}{\tilde{R}_1\tilde{R}_2} \end{bmatrix}, \quad |\tilde{\mathbf{S}}| = (S^\infty)^2, \quad \tilde{\Delta}_1 = 1 + \frac{(S^\infty)^2}{\tilde{R}\tilde{R}_2} + \frac{\tilde{S}_1}{\tilde{R}_1} + \frac{\tilde{S}_2}{\tilde{R}_2}. \tag{27}$$

Three observations on (27) are made.

(i) If receivers having identical mobilities $\tilde{R}_1 = \tilde{R}_2 = \tilde{R}$ are coupled to a symmetric spine, the responses for the parallel and series systems are

$$\tilde{\mathbf{Y}}^C(\text{parallel}) = \frac{1}{1+\tilde{S}_1/\tilde{R}}\begin{bmatrix} \tilde{S}_1 & \tilde{S}_{12} \\ \tilde{S}_{21} & \tilde{S}_1 + \dfrac{(S^\infty)^2}{\tilde{R}} \end{bmatrix},$$

$$\tilde{\mathbf{Y}}^C(\text{series}) = \frac{1}{1+\tilde{S}_1/\tilde{R}}\begin{bmatrix} \tilde{S}_1 + \dfrac{(S^\infty)^2}{\tilde{R}} & \tilde{S}_{12} \\ \tilde{S}_{21} & \tilde{S}_1 \end{bmatrix}. \tag{28}$$

Thus, the responses of the parallel and series systems *differ* when the spine is a wave-bearing system, whereas section 3.2 showed that they are *identical* when the spine is a modal system.

(ii) If the symmetric spine is coupled to two identical receivers having mobility $2\tilde{R}$, the coupled response is

$$\tilde{\mathbf{Y}}^C = \frac{1}{1+(S^\infty)^2/4\tilde{R}^2 + \tilde{S}_1/\tilde{R}}\begin{bmatrix} \tilde{S}_1 + \dfrac{(S^\infty)^2}{2\tilde{R}} & \tilde{S}_{12} \\ \tilde{S}_{21} & \tilde{S}_1 + \dfrac{(\tilde{S}^\infty)^2}{2\tilde{R}} \end{bmatrix}. \tag{29}$$

This result differs from the responses of the parallel and series systems, whereas in section 3.2 it was the same as the responses of the parallel and series systems using the modal spine.

(iii) It is clear that to preserve the dominance of the spine in the coupled responses, the additional terms in the matrix and in the expression for $\tilde{\mathbf{\Lambda}}_1$ must be small. This can only be true if

$$\frac{S_x^\infty}{\tilde{R}_x} \ll 1, \tag{30}$$

where x is any location on the spine having characteristic mobility S_x^∞ to which the receiver with mobility $\tilde{R}_x$ is attached.

Equation (30) provides a simple criterion to ensure dominance of the spine. To quantify a limit for (30) it is useful to consider the ratio of the coupled input mobilities of the compound system [i.e., the term in the top left of the matrix in equation (22) or equation (27)] to the uncoupled input mobility of the spine [i.e., the term in the top left of the matrix in equation (10)]. These ratios can be expressed as a function of the ratio of the characteristic mobility of the receiver R^∞ to the characteristic mobility of the spine S^∞. The use of the receiver's characteristic mobility is reasonable if one assumes that the receivers have moderate or high modal overlap which is likely to be true for built-up thin-plate structures like car bodies which have surface damping treatments to raise the flexural wave loss factor. Then individual resonances of the receivers are unimportant and only the ratio R^∞/S^∞ is significant. For the modal model, the ratio of the coupled input mobility to the spine uncoupled input mobility is

$$\frac{\tilde{Y}_1^C}{\tilde{Y}_1^S}(\text{modal}) = \frac{1}{1 + 2/(R^\infty/S^\infty)} \tag{31}$$

For the wave-bearing model, the same ratio is

$$\frac{\tilde{Y}_1^C}{\tilde{Y}_1^S}(\text{wave bearing}) = \frac{1 + 2/(R^\infty/S^\infty)}{1 + [1/(R^\infty/S^\infty)]^2 + 2/(R^\infty/S^\infty)}. \tag{32}$$

These two equations are plotted in Figure 3 for the range $1 \leqslant R^\infty/S^\infty \leqslant 100$ (values less than unity are immediately inadmissible because they imply that the receiver is less mobile than the spine). The difference between the wave-bearing and modal models is $<10\%$ when $R^\infty/S^\infty \geqslant 10$, indicating that the coupled responses based on a modal spine will preserve the dominant spine motion and approximate to within 10% of the response of a practical wave-bearing structure provided the receiver's characteristic impedances are less than one-tenth that of the spine at each point of attachment x, i.e.,

$$\tilde{Z}_x^{R\infty} \leqslant \frac{1}{10}\tilde{Z}_x^{S\infty}. \tag{33}$$

Therefore, for successful application of the hybrid method to thin-plate structures like the box equation (33) must be satisfied wherever a receiver is attached to the spine. For the six-sided box the input impedance at the stiff joints is dominated by the impedance of

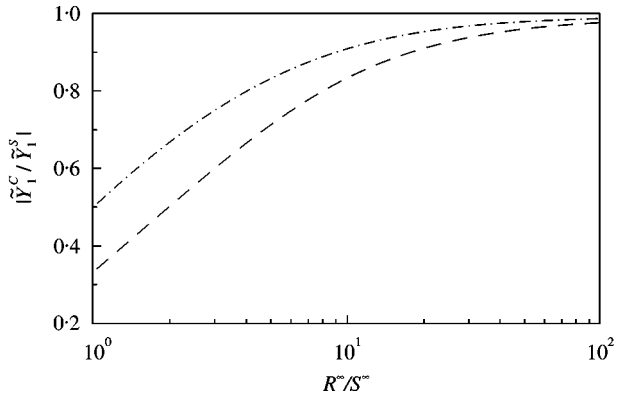

Figure 3. Ratio of the coupled input mobility of the compound system $\tilde{Y}_1^C$ to the input mobility of the uncoupled spine $\tilde{Y}_1^S$ as a function of the ratio of the characteristic input mobilities of the receiver and spine R^∞/S^∞ for spine structures whose mobilities are based on either modal (– – –) or wave-bearing (– · – · –) functions.

the plate driven in-plane, in which case the input impedance is

$$Z^{S\infty} = \left[\frac{\omega}{4}\left(\frac{1}{D_{LI}} + \frac{1}{D_S}\right)\right]^{-1}, \quad D_{LI} = \frac{Et}{(1-\nu^2)}, \quad D_S = \frac{Et}{2(1+\nu)}, \tag{34}$$

where D_{LI} is the in-plane stiffness and D_S is the shear stiffness of the plate [5]. Equation (4) defines the locally reacting impedance of a receiver modelled as a semi-infinite beam. Due to the different frequency dependencies of $Z^{S\infty}$ and $\tilde{Z}'_F$, equation (33) imposes a frequency limit on the hybrid method when applied to structures like the thin-plate box, over and above that dictated by equation (6). For the thin-plate box, equations (9) and (33) then give

$$L_R\tilde{Z}'_F \leqslant \frac{1}{10} Z^{S\infty}. \tag{35}$$

Thus, equations (9) and (35) reveal an interplay of the N_R parameter and the *product* of the parameters L_R and $\tilde{Z}_F$ as follows. The $L_R\tilde{Z}'_F$ product can be considered as determining the impedance of *individual* receivers needed to satisfy equation (35), while N_R dictates the *number* of receivers having the impedance $L_R\tilde{Z}'_F$ which are required to achieve a certain damping. It follows that N_R dictates the number of points on the spine at which receivers with impedance $L_R\tilde{Z}'_F$ must be attached.

3.4. POWER DISSIPATED BY THE RECEIVERS IN THE COMPOUND, PARALLEL AND SERIES SYSTEMS

The previous section examined the coupled response of the three systems shown in Figure 1 in order to define the N_R, L_R and $\tilde{Z}'_F$ parameters. This section analyses the power dissipated by the parallel and/or series receivers because this indicates more clearly how the *location* of the receivers relative to the location of the excitation force affects the damping of the spine. It also indicates how the receivers affect the response of a multi-modal spine as opposed to the single mode spine considered so far.

The time-averaged power injected into the compound system receivers can be found using the coupled mobility matrix (16) and the general relation $\bar{P} = \frac{1}{2}\mathrm{Re}\{\tilde{f}\tilde{v}^*\}$ to be

$$\bar{\bar{P}}^{R_1}(\text{parallel}) = \left|\frac{1}{\tilde{\Delta}_1}\left(\frac{\tilde{S}_1}{\tilde{R}_1} + \frac{|\tilde{\mathbf{S}}|}{|\tilde{\mathbf{R}}|}\right)\right|^2 \mathrm{Re}\{\tilde{R}_1\}, \quad \bar{\bar{P}}^{R_2}(\text{series}) = \left|\frac{1}{\tilde{\Delta}_1}\frac{\tilde{S}_{21}}{\tilde{R}_2}\right|^2 \mathrm{Re}\{\tilde{R}_2\}, \tag{36}$$

where the additional overbar indicates that these powers have been normalized by the mean-square excitation force $\frac{1}{2}|f_1|^2$. Henceforth, the time-averaged and mean-square force normalized powers injected into the receivers will be called *transmitted powers*. The following observations on equation (36) can be made.

(i) Both transmitted powers depend on $\tilde{\Delta}_1$. This indicates that *all* the receivers influence the power transmitted to *any one* receiver.
(ii) If the receiver mobilities are to satisfy equation (35), the transmitted powers will be quite small. This means that if the spine damping is to be raised appreciably it will be necessary to use a considerable number of receivers.
(iii) The power transmitted to the parallel receiver is strongly dependent on the ratio of the input mobilities of the receiver and the spine at the drive point. Even if the spine is lightly damped, its input mobility is never zero, so the parallel receiver will always draw power from the spine. This suggests that a single parallel receiver may be sufficient to damp the entire spine to some desired level if its impedance is sufficiently high yet conforms with equation (35).

The expressions for the transmitted powers in the parallel and series systems are easily obtained from the compound system results by letting $\tilde{R}_2 \to \infty$ and $\tilde{R}_1 \to \infty$ respectively. For the symmetric spine attached to receivers of identical mobility $\tilde{R}$, the powers transmitted to the parallel and series receivers are, respectively,

$$\bar{\bar{P}}^{R_1} = \left|\frac{\tilde{S}_1}{\tilde{S}_1 + \tilde{R}}\right|^2 \mathrm{Re}\{\tilde{R}\}, \quad \bar{\bar{P}}^{R_2} = \left|\frac{\tilde{S}_{12}}{\tilde{S}_1 + \tilde{R}}\right|^2 \mathrm{Re}\{\tilde{R}\}. \tag{37}$$

Three observations are made:

(i) If the multi-modal spine is anti-resonant its input mobility will be small. The parallel receiver will then be weakly coupled to the drive point and the amount of power transmitted to it will be smaller than at resonance.
(ii) If the multi-modal spine is anti-resonant and the value of the transfer mobility is that due to the "trough" between adjacent resonances, the coupling between the spine and a series receiver is better than between the spine and a parallel receiver. The power transmitted to the series receiver will then be *larger* than that transmitted to the parallel receiver.
(iii) If at some frequency the series receiver is attached at a vibration node, the coupling between the spine and the series receiver will be very weak, and the power transmitted to the series receiver will probably be less than the power transmitted to the parallel receiver.

In summary, all receivers affect the damping produced by every other receiver. A parallel receiver will only damp a multi-modal spine effectively when the spine is resonant, whereas a series receiver will damp a multi-modal spine at both resonance and anti-resonance provided it is not attached at a vibrational node. The latter behaviour is physically more realistic since practical structures dissipate energy at all frequencies, not just at resonance.

3.5. DAMPING THE SIX-SIDED BOX USING ONE OR TWO SEMI-INFINITE RECEIVERS

The previous sections presented theory which allowed some observations on the effect of the number and position of the receivers on the response of the spine. This theory will now be tested by damping the responses of the box shown in Figure 2 using one or two receivers. Figure 1 shows the compound, parallel and series systems consisting of the box coupled to one or two receivers. The receivers are semi-infinite which is reasonable if the flexural wave loss factor is quite high. In the parallel and series systems, the receiver width is twice the width of the two receivers used in the compound system. Therefore, in these three configurations, the total impedance of the receivers (i.e., the impedance which would arise were the two compound system receivers to be attached at the same point on the spine) is a constant. Thus, the damping produced by them should be identical according to (9). The following items cover the choice of receiver impedance, the admissible frequency range for the coupled responses and the damping which the receivers are expected to produce.

3.5.1. *Receiver impedance*

As mentioned previously, the large difference in the wavelength of the long and short waves in the structure means a locally reacting receiver impedance can be utilized. Thus, the receiver impedance is

$$\tilde{Z}_{FI} = \frac{m''_p L_R \omega}{2k_{FI}}(1 + \mathrm{j}), \tag{38}$$

where L_R is the width of the appropriate receiver in Figure 1.

3.5.2. *Admissible frequency range for the coupled responses*

Using equations (38) and (34) in equation (35) for the parallel and series systems in which the receiver width is 0·395 m, the admissible frequency range of the coupled responses is 1 kHz. For the compound system, this rises to 1·4 kHz because of the lower receiver impedance.

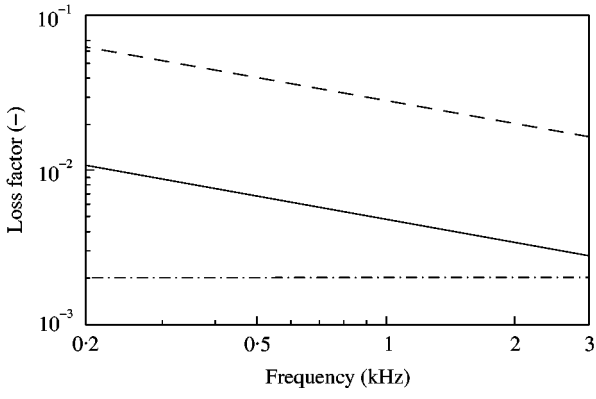

Figure 4. Loss factors for the coupled box and receiver configurations: ——, loss factor produced by receivers in Figure 1; – – –, loss factor produced by receivers in Figure 7 (see section 4); – · – · –, loss factor of lightly damped box.

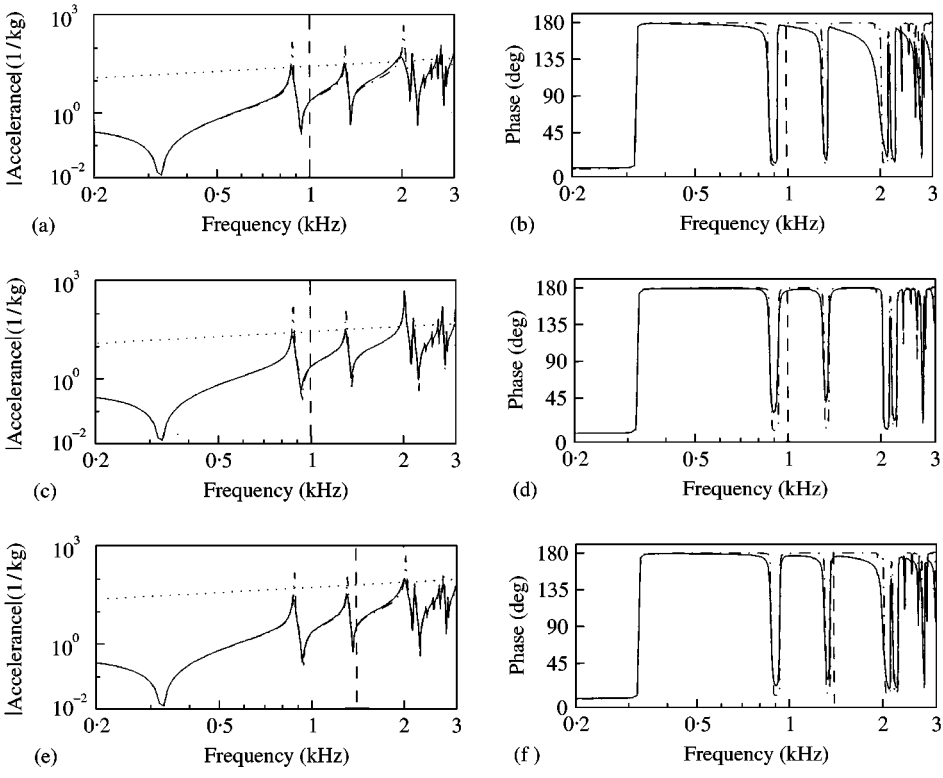

Figure 5. Input accelerance at point 1 in the z-direction for the lightly damped box coupled in the parallel, series and compound configurations of Figure 1: (a, b) parallel system; (c, d) series system; (e, f) compound system: ——, coupled response; – · – · –, response of box without receivers; · · · ·, input accelerance of receiver; – – –, frequency limit for coupled responses according to equation (35).

3.5.3. *Loss factor produced by attaching the receivers to the box*

Figure 4 shows the loss factor calculated using equation (9) which is produced by coupling the receivers to the spine. It can be seen that the additional damping increases the box damping considerably at low frequencies. The additional damping falls with $\sqrt{\omega}$ due to the frequency dependence of the receiver impedance in equation (38).

3.5.4. *Coupled responses for the three systems*

Figure 5 shows the magnitude and phase of the input accelerances at point 1 in the z-direction for the systems in Figure 1, while Figure 6 shows the transfer accelerances at point 2 in the z-direction. Both figures show the input accelerances of the relevant receivers derived from the inverse of equation (38). Some observations are now made.

(i) In both Figures 5 and 6, the peak levels of the two well-spaced resonances at 880 and 1300 Hz are virtually identical for all three configurations as expected from the previous theory. The predicted loss factors at these frequencies from Figure 4 are shown in Table 1 together with the values calculated for these two resonances using the Argand diagram technique. The values from the coupled responses are rather higher than those predicted. Strictly, the resonance at 1300 Hz is not admissible for the parallel and series systems.

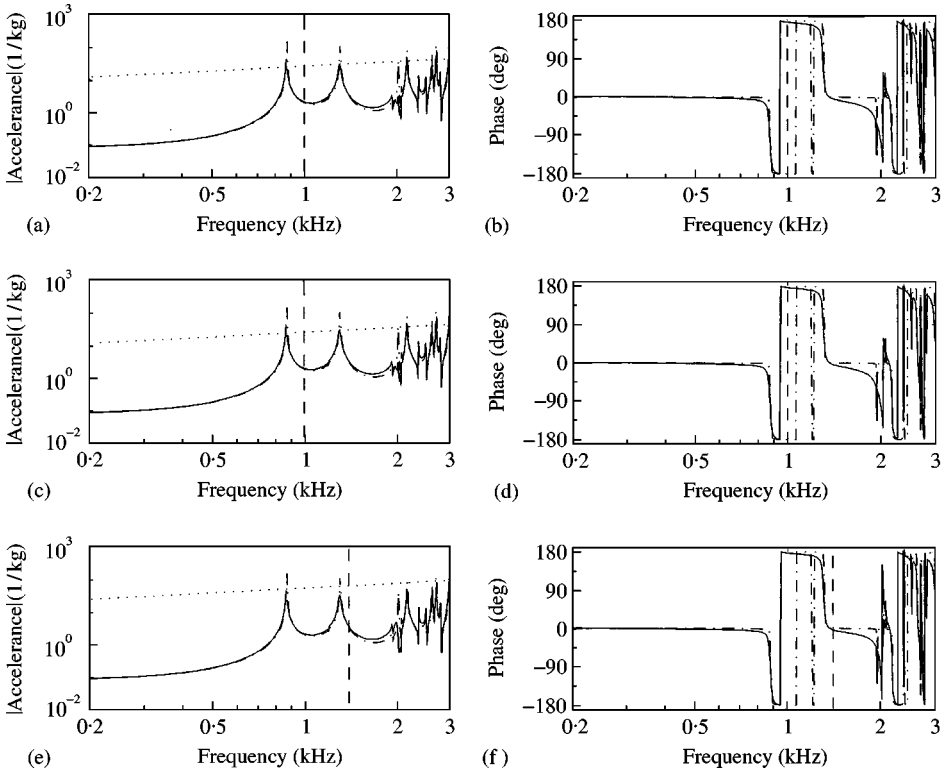

Figure 6. Transfer accelerance at point 2 in the z-direction for the lightly damped box coupled in the parallel, series and compound configurations of Figure 1: (a, b) parallel system; (c, d) series system; (e, f) compound system: ——, coupled response; –·–·–, response of box without receivers; ····, input accelerance of receiver; – – –, frequency limit for coupled responses according to equation (35).

TABLE 1

Predicted and estimated loss factors for the two lowest resonances produced by coupling the lightly damped perspex box to receivers as in Figure 1

Resonance frequency	Loss factor predicted by Figure 4	Loss factor estimated from the coupled input response		
		Parallel system	Series system	Compound system
877	0·005	0·011	0·011	0·011
1304	0·004	0·015	0·015	0·015

(ii) The peak level of the compound system response at these resonances is below that of the receiver accelerances indicating that all the receivers influence the coupled response as indicated in section 3.4.

(iii) At 2 kHz (which is well above the admissible frequency range of the coupled responses) the magnitudes of the three responses differ significantly. For the parallel and compound systems the coupled response is very close to the level of the receiver accelerance. For the series system, the peak level has not altered from that of the uncoupled spine. Therefore, the series receiver acting at point 2 in the z-direction must be attached at a vibration node for this mode.

(iv) The phase curve in Figure 5(b) shows that the parallel receiver only damps the response at the spine resonances, producing an unusual phase curve which is particularly noticeable around the resonances at 880 and 1300 Hz. In contrast, the phase curve for the series receiver in Figure 5(d) has a much more typical appearance.

Overall it is considered that these results support the theory. Thus, to achieve a certain damping of the spine, the impedance of the receivers can be applied at a single point on the spine, or it can be distributed to a number of points on the spine, provided the total impedance remains unchanged. The advantage of splitting the total impedance amongst many points is that the bandwidth over which the coupled response is admissible increases. However, if the increase in damping is to be uniform across all modes, the receivers must not be attached at any vibrational nodes.

Intuitively, one can remark that the greater the number of points on the spine which are coupled to receivers, the greater is the likelihood of the spine modes being damped. The disadvantage of this approach is that more spine frequency response functions are required which increases the numerical expense. Thus, it would appear that successful application of the hybrid method to built-up thin-plate structures like car bodies depends on the correct choice of the locations for the receivers. The next section addresses this matter in more depth.

4. RESPONSE OF THE SPINE WHEN ATTACHED TO LARGE NUMBERS OF RECEIVERS WITH CONSTANT ADDITIONAL DAMPING

To investigate more fully the effect of the receiver locations on the coupled responses, consider Figure 7 which shows the box attached to two slightly different configurations of six receivers. In Figure 7(a), a receiver is attached at point 3 and is driven in the x-direction by the spine, whereas in Figure 7(b) this receiver has been moved to point 4 and is driven in the z-direction by the spine. All the receivers have widths the same as the wider parallel and series receivers in Figure 1. Figure 4 shows the damping which should be produced by these six receivers, as predicted using equation (9). The damping produced by these receivers is of course higher than those shown in Figure 1, but because their width is the same as the width of the parallel and series receivers the admissible frequency range for the coupled responses is still 1 kHz.

To calculate the coupled response for the box attached to the six receivers, the spine and receiver mobilities are coupled using the procedure of section 3.1, but of course the matrices are now of order 6. Figure 8 compares the coupled responses for the two configurations of 6 receivers at 3 points as follows: the input response at point 1 in the z-direction [Figure 8(a) and 8(b)], the transfer response at point 2 in the z-direction [Figure 8(c) and 8(d)], and the input response at point 4 in the z-direction [Figure 8(e) and 8(f)]. Table 2 shows the predicted loss factors from equation (9) at a number of resonances of the coupled responses together with values obtained from the coupled responses using an Argand diagram. The following observations are made.

(i) The input responses at point 1 of both configurations are very similar. In comparison with Figure 2, the resonances of the coupled systems are slightly lower than those of the uncoupled spine due to the additional mass of the receivers.
(ii) In both configurations, the resonance at 866 Hz is damped identically. As shown in Table 2, the actual loss factor determined using an Argand diagram is 0·030 which is near the predicted value of 0·025.
(iii) For the input response at point 4 [Figure 8(e)], the resonance at 920 Hz has not been damped at all using the configuration of Figure 7(a), yet is damped much more using

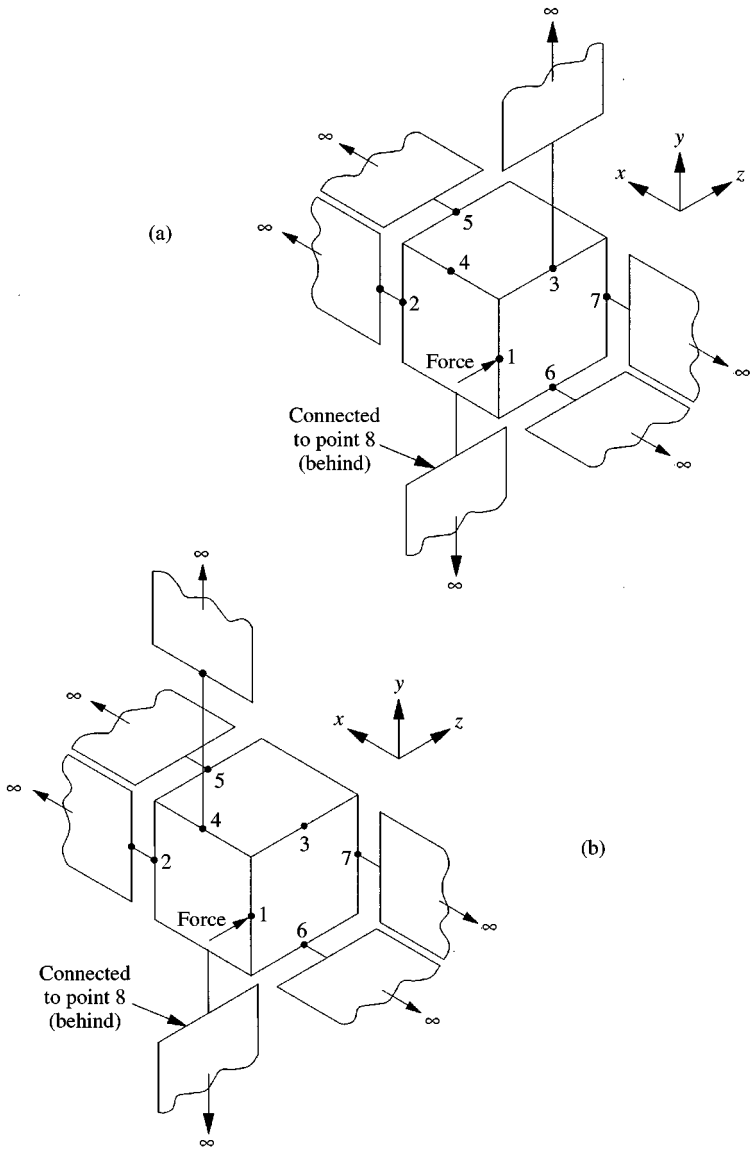

Figure 7. The box attached to six fullwidth semi-infinite receivers connected in two configurations: (a) receiver present at point 3; (b) receiver moved from points 3 to 4.

the configuration of Figure 7(b). This shows that moving just one receiver can have a significant effect on the coupled response.

These results show that even an apparently modest number of receivers is not necessarily sufficient to produce damping which is uniform in both frequency and spatial terms over the entire structure, as is to be expected for a practical wave-bearing structure. Clearly this problem is due to the modal method used to calculate the spine response.

In an attempt to produce a response which is uniformly damped in both frequency and spatial terms, Figure 9 shows the coupled responses for the three points considered in Figure 8 but with 24 receivers attached uniformly over the box. The receivers are attached

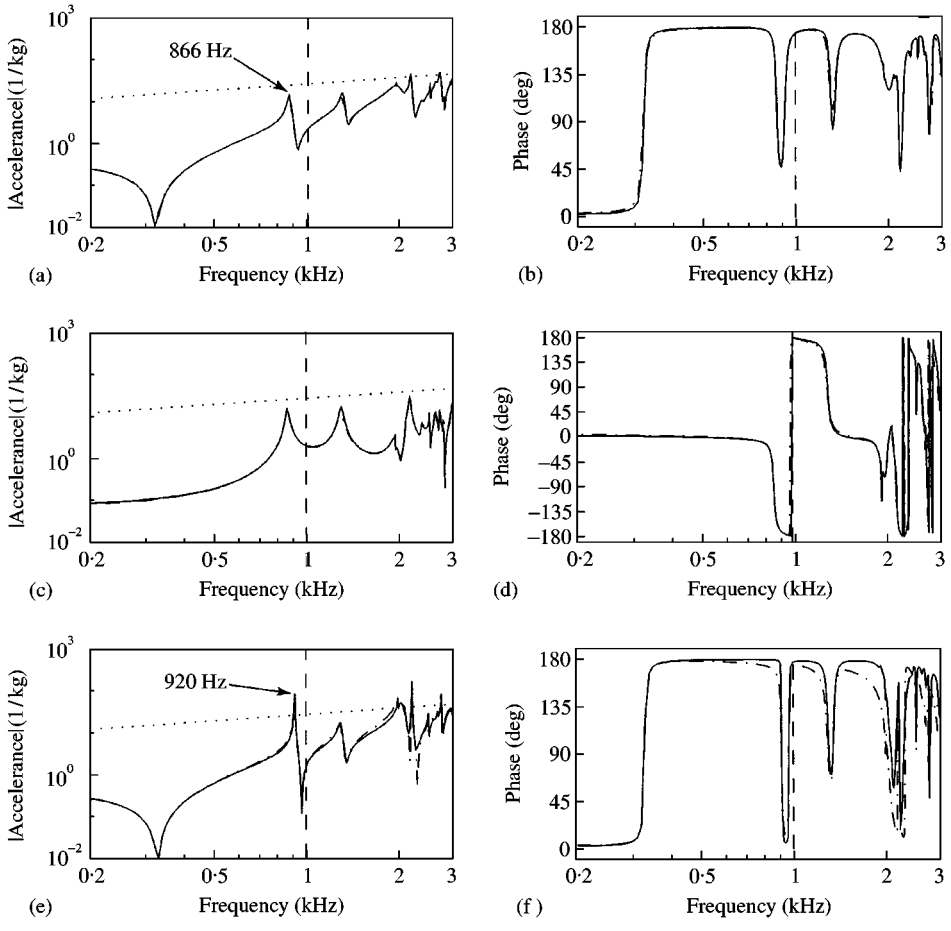

Figure 8. Response of the box attached to the six receivers of Figure 7(a) (——) and Figure 7(b) (– · – · –): (a, b) modulus and phase of input accelerance at point 1 in the z-direction; (c, d) modulus and phase of transfer accelerance at point 2 in the z-direction; (e, f) modulus and phase of input accelerance at point 4 in the z-direction; · · · ·, typical input accelerance of receiver; – – –, frequency limit for hybrid method.

at the mid-point of every joint of the box in the manner of Figure 7. However, the receiver widths are reduced to one-quarter of those shown in Figure 7 so that the total impedance of the receivers remains the same as in Figure 7. Consequently, the additional damping is the same as shown in Figure 4. However, because the individual impedances are smaller, the admissible bandwidth increases to 2·3 kHz. For comparison, the responses for the configuration of Figure 7(a) from Figure 8 are reproduced in Figure 9. Some observations of Figure 9 are as follows.

(i) In Figure 9(a) and 9(b) the loss factor of the resonances at 866 and 1294 Hz are close to 0·023 and are approaching the theoretical values shown in Table 2, but the loss factor of the resonance at 1985 Hz is 0·038 which is twice the theoretical value of 0·019. Therefore, equation (9) is not always reliable for predicting the additional damping.

(ii) For the transfer accelerance at point 2, the response is damped at the 866 and 1294 Hz resonances as well as in the "trough" between these resonances.

TABLE 2

Theoretical and actual loss factors for the different spine/receiver configurations

Number of receivers	Maximum admissible frequency	Coupled response figure	Resonance frequency from coupled response (Hz)	Predicted loss factor from Figure 4	Actual loss factor from coupled input responses	Difference relative to predicted loss factor (%)
			f_n	η	η	
6 as in Figure 7(a)	1000	8(a)	866	0·030	0·025	−17
		8(e)	920	0·029	0·002	−93
6 as in Figure 7(b)	1000	8(a)	866	0·030	0·023	−23
		8(e)	920	0·029	0·016	−45
24 in the manner of Figure 7	2300	9(a)	866	0·030	0·023	−23
		9(e)	910	0·029	0·022	−24
		9(a)	1294	0·025	0·023	−8
		9(e)	1985	0·019	0·038	+100

(iii) For the input response at point 4, the resonance at 910 Hz has now been damped much better than by the receivers in Figure 7(a). Table 2 shows that its loss factor of 0·022 is close to the predicted value.

Overall, these results suggest that large numbers of small receivers are required to reliably produce frequency response functions having the form to be expected of practical wave-bearing structures.

5. USE OF THE HYBRID METHOD TO PREDICT THE FLEXURAL VIBRATIONS IN THE ACTUAL SIX-SIDED BOX

The previous sections examined the effect of damping a spine with semi-infinite receivers in an effort to define the parameters in equation (9). Semi-infinite receivers are appropriate if the flexural wave loss factor is quite high, but if this loss factor is low the flexural waves may create resonances in the structure which the receivers should attempt to model. In such cases the receivers need to have finite length. Thus in this section, the hybrid method is used to couple finite and therefore resonant receivers to a spine, and the method is applied to predict the flexural response of three of the sides of the actual structure whose long wave response was considered in reference [5]. The predictions are compared with laboratory measurements.

5.1. COUPLED MOBILITY MATRIX FOR THE COMPOUND SYSTEM USING A SINGLE FINITE RECEIVER

If the ends of a single finite length receiver are attached to spine points 1 and 2 in Figure 1, the receiver mobility matrix becomes

$$\begin{bmatrix} \tilde{v}_1^R \\ \tilde{v}_2^R \end{bmatrix} = \begin{bmatrix} \tilde{R}_1 & \tilde{R}_{12} \\ \tilde{R}_{21} & \tilde{R}_2 \end{bmatrix} \begin{bmatrix} \tilde{f}_1^R \\ \tilde{f}_2^R \end{bmatrix}, \tag{39}$$

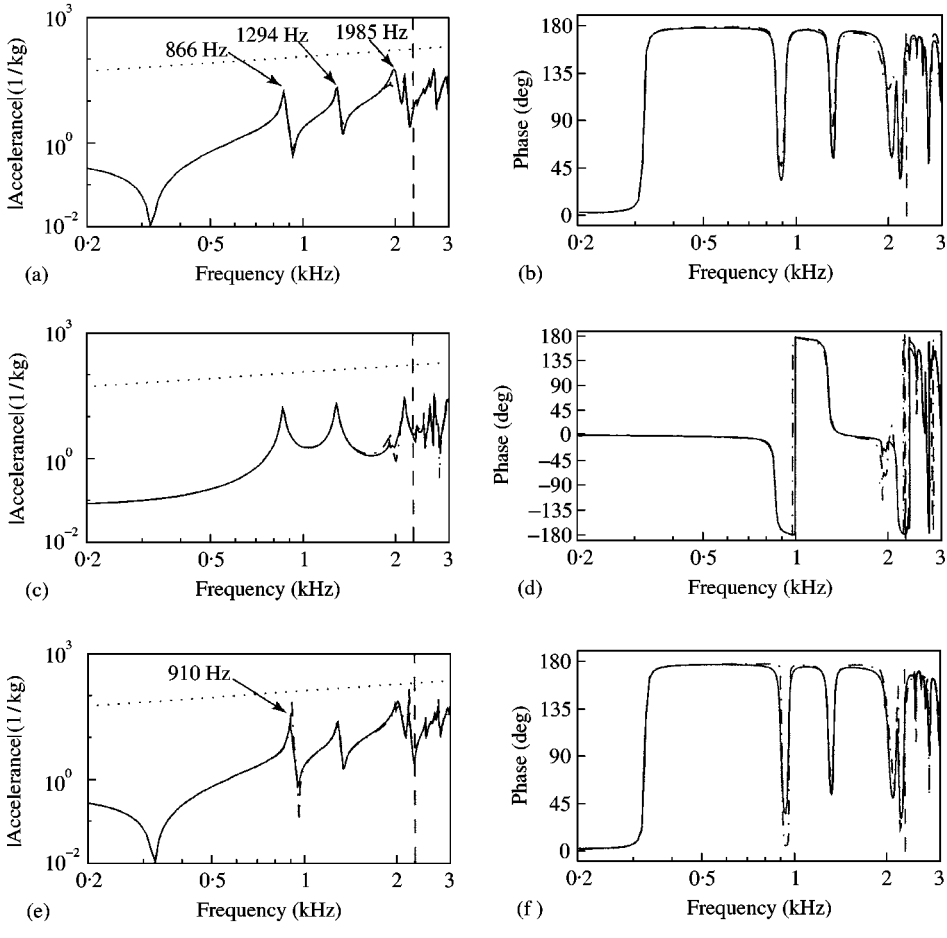

Figure 9. Response of the box attached to the six receivers of Figure 7(a) (– · – · –) or 24 receivers, one at the mid-point of every side in Figure 7 (——): (a, b) modulus and phase of input accelerance at point 1 in the z-direction; (c, d) modulus and phase of transfer accelerance at point 2 in the z-direction; (e, f) modulus and phase of input accelerance at point 4 in the z-direction; · · · ·, typical input accelerance of receiver used in the configuration of 24 receivers; – – –, frequency limit for hybrid method using 24 receivers.

where $\tilde{R}_{12}$, $\tilde{R}_{21}$ are the transfer mobilities between its ends. Using this mobility matrix in the analysis of section 3.1 produces the following coupled mobility matrix (after some manipulation):

$$\tilde{\mathbf{Y}}_C = \frac{1}{\tilde{\Delta}_2}\begin{bmatrix} \tilde{S}_1 + \tilde{R}_1\dfrac{|\tilde{\mathbf{S}}|}{|\tilde{\mathbf{R}}|} & \tilde{S}_{12} + \tilde{R}_{12}\dfrac{|\tilde{\mathbf{S}}|}{|\tilde{\mathbf{R}}|} \\ \tilde{S}_{21} + \tilde{R}_{21}\dfrac{|\tilde{\mathbf{S}}|}{|\tilde{\mathbf{R}}|} & \tilde{S}_2 + \tilde{R}_2\dfrac{|\tilde{\mathbf{S}}|}{|\tilde{\mathbf{R}}|} \end{bmatrix}, \quad |\tilde{\mathbf{R}}| = \tilde{R}_1\tilde{R}_2 - \tilde{R}_{12}\tilde{R}_{21}. \tag{40}$$

Here, $|\tilde{\mathbf{S}}|$ is as before and $\tilde{\Delta}_2$ is

$$\tilde{\Delta}_2 = 1 + \frac{|\tilde{\mathbf{S}}|}{|\tilde{\mathbf{R}}|} + \frac{\tilde{S}_1\tilde{R}_2}{|\tilde{\mathbf{R}}|} + \frac{\tilde{S}_2\tilde{R}_1}{|\tilde{\mathbf{R}}|} + 2\frac{\tilde{S}_{12}\tilde{R}_{12}}{|\tilde{\mathbf{R}}|}. \tag{41}$$

The following observations can be made.

(i) In comparison with the coupled mobility matrix of equation (17), the matrix here features additional off-diagonal terms, and the parameter $\tilde{\mathbf{\Delta}}_2$ has additional terms over $\tilde{\mathbf{\Delta}}_1$ in equation (17). These new terms will introduce additional resonances into the coupled response as expected.

(ii) If the modal overlap in the receivers becomes high, i.e., if $\eta_R k_{FI} L_y \gg 1$ (where L_y equals the length of the receiver which matches the distance between the two spine points 1 and 2) the receiver input mobilities tend to the characteristic mobility, the transfer mobilities becomes small and the coupled mobility matrix reverts to equation (17). Thus, the response of the spine coupled to a finite receiver will only differ significantly from the response when coupled to two independent semi-infinite receivers if the receiver modal overlap is low. In other respects, the response of the spine coupled to a finite receiver will follow the characteristics already noted in section 3, and equation (33) can still be expected to determine the magnitude of the receiver impedance relative to that of the spine.

5.2. RECEIVER IMPEDANCES, LOSS FACTOR AND ADMISSIBLE BANDWIDTH FOR THE RECEIVERS WHICH ARE TO BE COUPLED TO THE ACTUAL BOX

Figure 10 shows the box from reference [5] attached to 12 finite length receivers, each one being attached at two points to the box. The receivers have a length equal to the length of

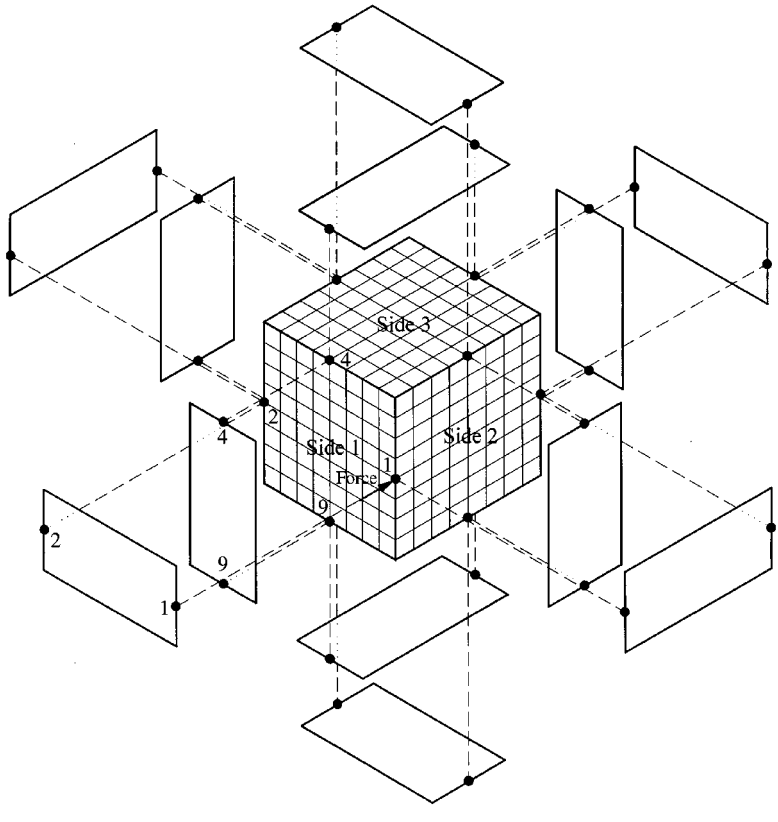

Figure 10. The box attached to 12 finite length halfwidth receivers. The box is driven by a force as shown.

the box side which they span. Their input impedances $\tilde{Z}_1$ and transfer impedances $\tilde{Z}_{12}$ are calculated using [7]

$$\tilde{Z}_1 = \frac{m''_p L_R \omega}{2k_{FI}} \left(\frac{1+\tilde{\alpha}}{1-\tilde{\alpha}} + \mathrm{j} \right), \quad \tilde{Z}_{12} = -\frac{m''_p L_R \omega}{k_{FI}} \left(\frac{\sqrt{\tilde{\alpha}}}{1-\tilde{\alpha}} \right), \quad \tilde{\alpha} = \mathrm{e}^{-\mathrm{j}2\tilde{k}_{FI} L_y}, \tag{42}$$

where L_R is the appropriate width. The receiver widths were determined in the following manner. In the actual structure the flexural wave loss factor is the same as the in-plane wave loss factor, both having values of 0·05. Thus, the 12 receivers shown in Figure 10 must provide a loss factor of about this value. From Figure 4 it can be seen that the receivers of Figure 7 provide a loss factor of around 0·03 at 1 kHz, which is roughly half the desired flexural wave loss factor. Therefore, for the 12 finite receivers (which act like 24 receivers because each is attached at two points on the box) to have twice the damping of the six receivers, each must be half as wide as the six receivers of Figure 7. The 12 finite receivers will therefore produce a loss factor of around 0·06 at 1 kHz, and the frequency limit for the hybrid method calculations will be 1400 Hz using equation (35).

The transfer impedance in equation (42) assumes that the receivers when not connected to the spine have a simple support at their undriven end, a condition which is necessary for the transfer impedance to be non-zero even though it may not be totally accurate. However, since this boundary condition affects the precise resonances and anti-resonances of the receivers it is only of great importance when the structure is driven using narrowband excitation. It is less significant for broadband excitation.

Figure 11 shows the input and transfer impedances of the receivers calculated using equation (42). There are three impedances having slightly different resonance and anti-resonance frequencies because the box has slightly different side lengths in the three orthogonal directions. Figure 12 shows the loss factor predicted using equation (9) which shows numerous peaks and troughs because of the peaks and troughs in the real part of the receiver input impedances. The admissible bandwidth using equation (35) is 1400 Hz.

5.3. PREDICTION AND MEASUREMENT OF THE MEAN-SQUARE FLEXURAL ACCELERATION OF THE BOX

This section shows how the receivers are used to predict the spatially averaged mean-square flexural response of the box sides, and how the same quantity is measured on the box used in reference [5].

To calculate the mean-square flexural acceleration of the sides of the box, it is necessary to determine the transmitted powers for those receivers which can be considered as modelling the flexural response of the individual box sides. Examining Figure 10, one can consider that the flexural response of the side bounded by nodes 1, 2, 4 and 9 is modelled by the two receivers connected between these same nodes (i.e., one connected between nodes 1 and 2 and the other connected between nodes 4 and 9). The hybrid method provides the total time-averaged power $\bar{P}_{tot}$ injected by the spine into both receivers at both ends. The mean-square acceleration $\|\ddot{x}\|^2$ of these two receivers is therefore

$$\|\ddot{x}\|^2 = \frac{\omega \bar{P}_{tot}}{\eta_R M_{tot}}, \tag{43}$$

where M_{tot} is the total mass of the two receivers.

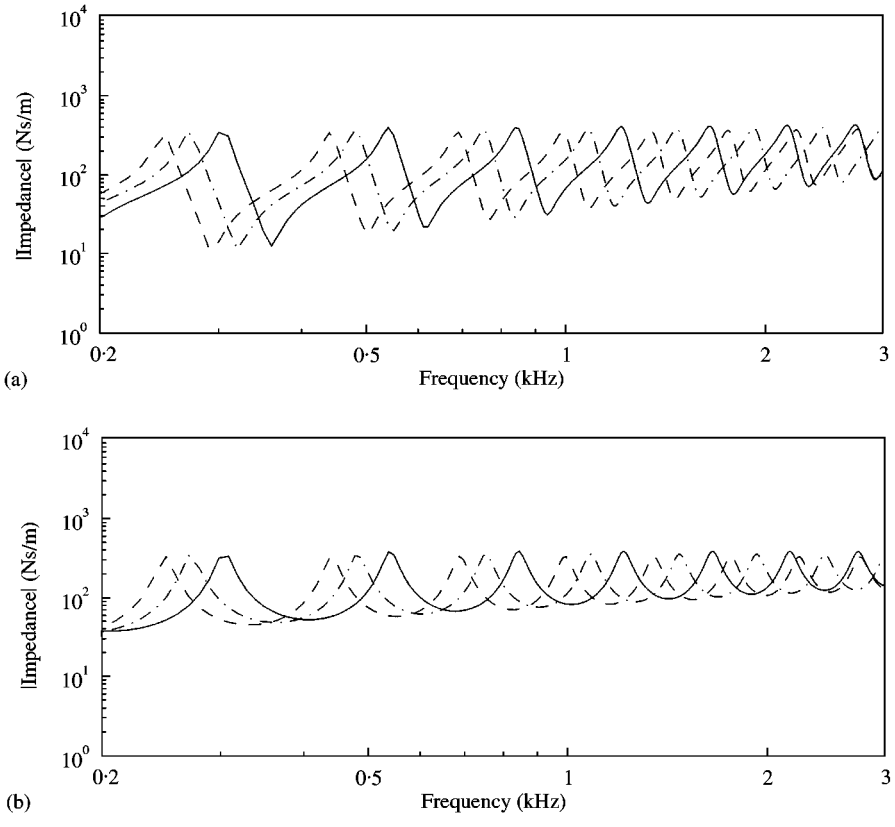

Figure 11. Impedances of the finite length halfwidth receivers coupled to the box as shown in Figure 10: (a) input impedances, and (b) transfer impedances having lengths as follows: ——, 0·373 m; – · – · –, 0·395 m; – – –, 0·413 m.

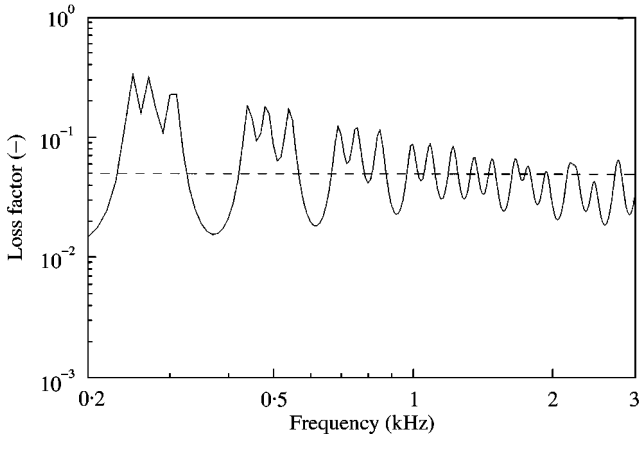

Figure 12. Loss factors for the box coupled to 12 finite halfwidth receivers: ——, loss factor produced by receivers; – – –, loss factor of in-plane waves in box.

To measure the spatially averaged mean-square flexural response of the both sides, the box was excited at point 1 using a shaker [5]. A single miniature accelerometer was fixed to a randomly selected point on the box using beeswax and the transfer accelerance to this point was measured. The accelerometer was moved to another randomly selected location and the process repeated. In total, 15 measurements were made on each of three sides (selected at random) shown in Figure 10.

5.4. COUPLED RESPONSES FOR THE SPINE ATTACHED TO THE FINITE RECEIVERS

The hybrid method was used to calculate the response of the lightly damped perspex box coupled to the 12 finite length receivers. Figures 13 and 14 compare the hybrid method results with the measured input and transfer accelerances at points 1 and 2, respectively, on the actual box from [5]. As expected from equation (40), the coupled responses exhibit a few additional resonances due to the resonances of the receivers. The additional mass loading of the receivers has reduced the coupled resonance frequencies, but they do not appear to have altered the box response greatly because the spine is already quite well damped.

5.5. MEAN-SQUARE ACCELERATION OF THE BOX SIDES

Figure 15 shows the one-third octave band averaged predicted and measured mean-square accelerations of the three box sides indicated in Figure 10 together with

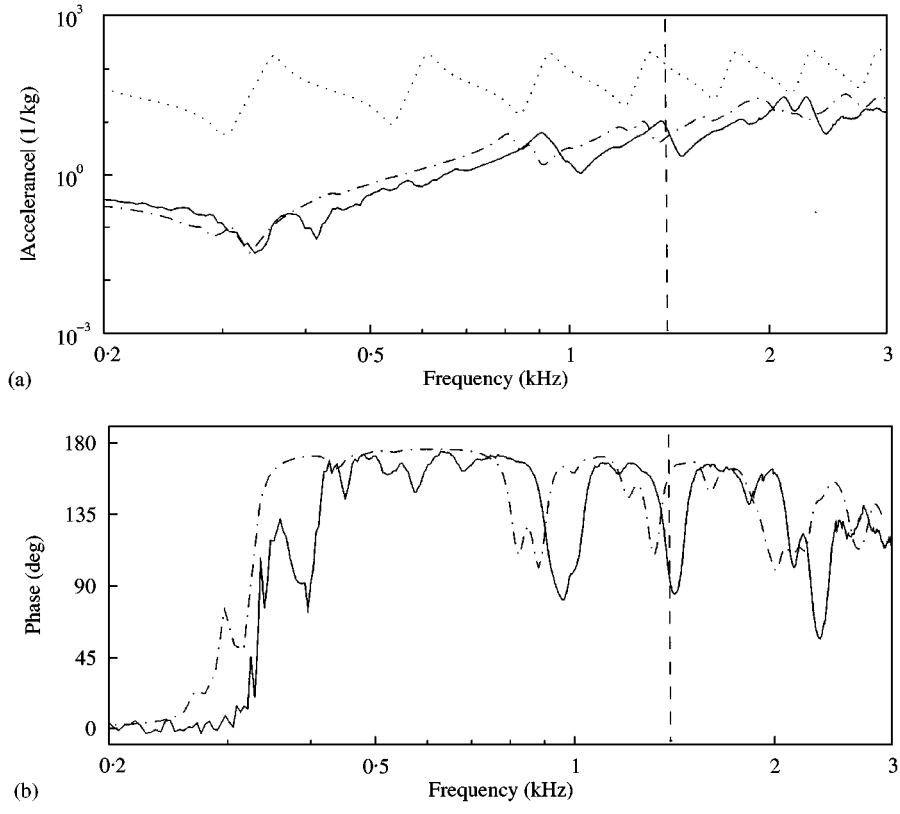

Figure 13. Input accelerance at point 1 in the z-direction for the box attached to 12 finite length halfwidth receivers: ——, measurement; – · – · –, hybrid method; · · · ·, typical input accelerance of receiver; – – –, frequency limit for hybrid method.

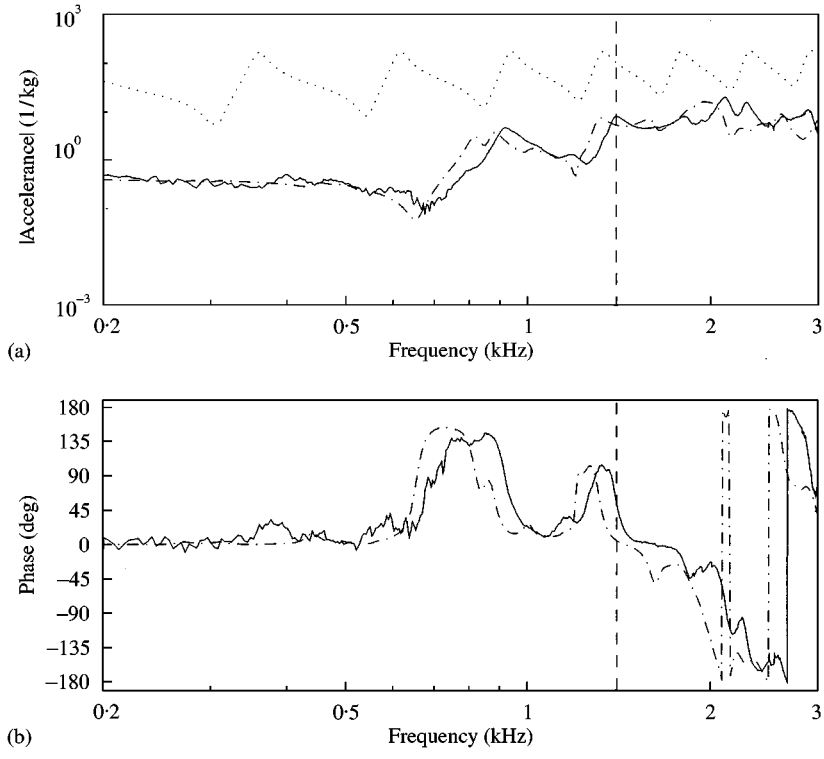

Figure 14. Transfer accelerance at point 2 in the z-direction for the box attached to 12 finite length halfwidth receivers: ——, measurement; –·–·–, hybrid method; ····, typical input accelerance of receiver; – – –, frequency limit for hybrid method.

± 3 dB confidence limits for the measured mean. The predictions are only valid up to 1400 Hz. The following points are noted.

(i) The predicted and measured mean-square accelerations for side 1 agree modestly at both the frequency average and peak levels. There is little agreement between individual peaks and troughs but this is not expected on account of the arbitrarily selected boundary condition at the undriven end of the receivers. However, from a practical standpoint it is considered more important that an estimate of the peak level is predicted.

(ii) In the case of side 2 the predicted mean-square acceleration underestimates the measurement by approximately one order of magnitude and lies far outside the ± 3 dB confidence limits for the measured mean. The prediction is therefore a poor estimate of the measurement at this confidence level.

(iii) For side 3, the prediction underestimates the measurement between 1200 and 1400 Hz by more than an order of magnitude and lies well outside the ± 3 dB confidence limits, but below 1200 Hz the two curves are in much better agreement.

Whilst the agreement between the predictions and measurements is only modest, the results suggest that the hybrid method applied to this type of structure does have some merit. The only modest agreement between the predictions and measurements may be a result of the choice of the receiver impedance in equation (42), which is itself based on equation (4) fundamentally. Other impedances (e.g., those which accommodate continuous rotation of the interconnected plates) could be tried to improve the results.

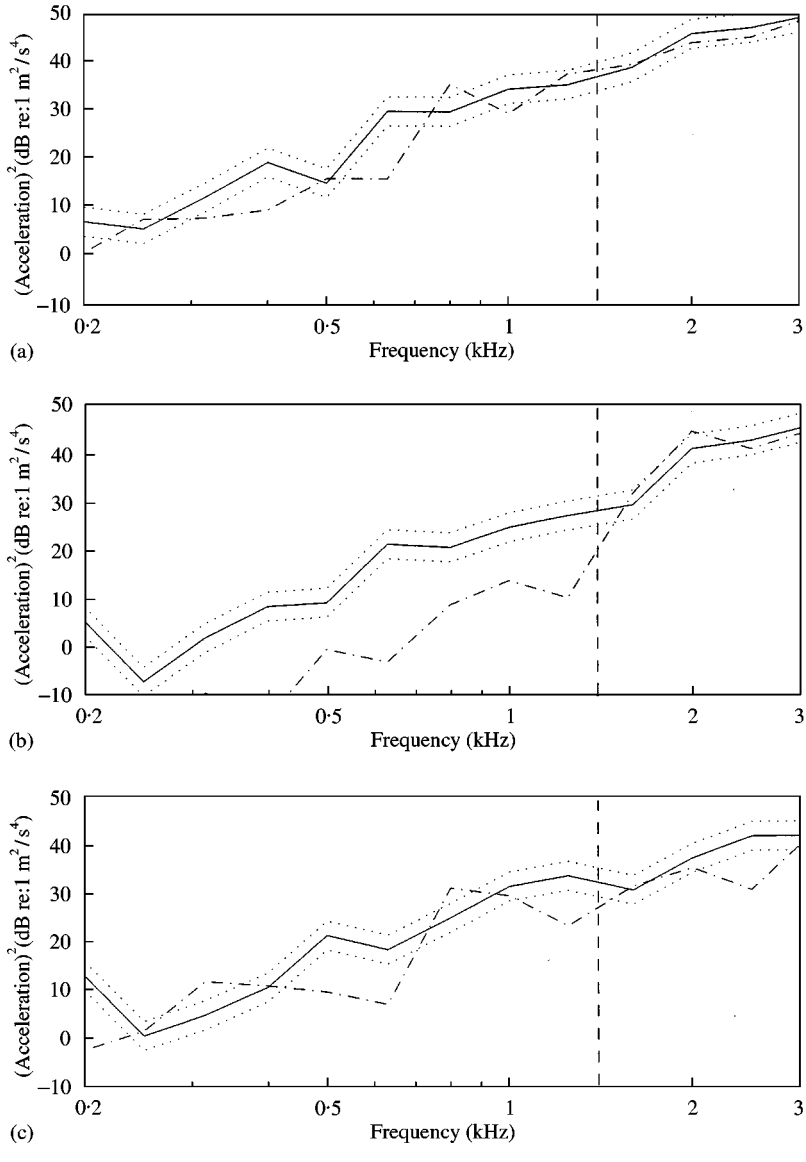

Figure 15. One-third octave band mean-square acceleration levels for the three sides of the box: ——, measurement; ····, ±3 dB confidence limits for the measurements; –·–·–, hybrid method; – – –, frequency limit for hybrid method: (a) side 1, (b) side 2, (c) side 3.

6. CONCLUDING REMARKS

Consideration has been given to applying the hybrid method of Grice and Pinnington [1, 3] to model the short-wavelength flexural vibrations of built-up thin-plate structures whose long-wavelength in-plane vibrations can be analyzed using the technique of Grice and Pinnington [5]. Essentially, the hybrid method can be applied to these structures by coupling analytical impedances ("receivers") to the long-wavelength model of the structure (the "spine"). The receivers model the impedance of flexural waves generated in the structure

when the long waves impinge on its joints, absorb power from the spine and thereby increase its damping.

Analytical and numerical analyses have been used to identify the parameters of the receivers. Although these cannot be quantified exactly, the following main points are concluded:

(i) The additional damping produced by attaching the receivers to the spine is proportional to their total impedance.
(ii) If the spine is based on a modal summation as in reference [5], each well-spaced mode can be damped to the same degree if the receivers are attached at any one point (i.e., at or away from the drive point) or distributed among many points, provided the total receiver impedance remains a constant.
(iii) If the spine is modelled using a wave-bearing model (as in the case of practical structures) its response when coupled to receivers differs from that of the modal spine coupled to the same receivers.
(iv) The modal and wave-bearing models yield similar responses when coupled to receivers provided the receiver characteristic impedances are at least one order to magnitude less than that of the spine at each attachment point. This condition also defines a frequency limit on the coupled responses.
(v) A greater number of receivers having smaller individual impedances increases the admissible bandwidth of the coupled responses.
(vi) If a receiver is attached at a vibration node of any spine mode, it will not damp the mode.

Numerical examples using the six-sided box from [5] have shown that in general the hybrid method is most reliable when a large number of small receivers are attached to the spine, albeit with greater numerical expense. The method has been used to predict the spatially averaged mean-square vibration of three sides of the box. These predictions have compared modestly with measurements. Further work is anticipated to investigate whether different receiver impedances yield more accurate predictions.

REFERENCES

1. R. M. GRICE and R. J. PINNINGTON 2000 *Journal of Sound and Vibration* **230**, 824–849. A method for the vibration analysis of built-up structures, Part I: introduction and analytical analysis of the plate-stiffened beam.
2. H. KUTTRUFF 1979 *Room Acoustics*. Applied Science: second edition.
3. R. M. GRICE and R. J. PINNINGTON 2000 *Journal of Sound and Vibration* **230**, 851–875. A method for the vibration analysis of built-up structures, Part II: analysis of the plate-stiffened beam using a combination of finite element analysis and analytical impedances.
4. U. CARLSSON 1993 *Ph.D. Thesis, Department of Vehicle Engineering, Royal Institute of Technology, Stockholm, Sweden*. Mechanical mobility: a tool for the analysis of vibrations in mechanical structures.
5. R. M. GRICE and R. J. PINNINGTON 2000 *Journal of Sound and Vibration* **232**, 449–471. Vibration analysis of a thin-plate box using a finite element model which accommodates only in-plane motion.
6. M. PETYT 1990. *Introduction to Finite Element Vibration Analysis*. Cambridge: Cambridge University Press.
7. R. J. PINNINGTON and D. LEDNIK 1996. *Journal of Sound and Vibration* **189**, 265–287. Transient energy flow between two coupled beams.

APPENDIX A: NOMENCLATURE

A	a constant (dimensionless)
b	width (m)
D	plate stiffness (Nm^2)

E	Young's modulus of elasticity (N/m^2)
$\bar{E}$	total time-averaged energy of vibration (Nm)
f	circular frequency (Hz); force (N)
j	$\sqrt{-1}$
k	wavenumber (m^{-1})
L	length (m)
m''_p	mass per unit area of a plate (kg/m^2)
M	mass (kg)
N	integer (dimensionless)
$\bar{P}$	time-averaged power (Nm/s)
$\bar{\bar{P}}$	mean-square force normalized time-averaged power (Nm/s)
R	mobility of a *receiver* structure (m/s/N)
$\mathbf{R}$	mobility matrix of a *receiver* structure (m/s/N)
S	mobility of a *spine* structure (m/s/N)
$\mathbf{S}$	mobility matrix of a *spine* structure (m/s/N)
t	thickness (m)
v	velocity (m/s)
x, y, z	Cartesian co-ordinates (m)
$\ddot{x}$	acceleration (m/s^2)
Y	structural mobility (m/s/N)
$\mathbf{Y}$	structural mobility matrix (m/s/N)
Z	structural impedance (Ns/m)
Z'	structural impedance per unit length (Ns/m^2)
$\mathbf{Z}$	structural impedance matrix (Ns/m)
α	travelling wave attenuation coefficient (dimensionless)
η	structural loss factor (dimensionless)
ν	Poisson's ratio (dimensionless)
ρ	density (kg/m^3)
ω	radian frequency (rad/s)
$\mathbf{\Delta}$	matrix parameter (dimensionless)
Φ	mode shape value